The Effect of Head Orientation and Personalized Ventilation on Bioaerosol Deposition from a Cough

Running title: Head orientation & PV role in deposition

Jingcui Xu[1,2], Cunteng Wang[1,3], Sau Chung Fu[3], Christopher Y. H. Chao[3,4]

[1]Department of Mechanical and Aerospace Engineering, The Hong Kong University of Science and Technology, Hong Kong, China

[2]Department of Civil and Environmental Engineering, The Hong Kong Polytechnic University, Hong Kong, China

[3]Department of Mechanical Engineering, The University of Hong Kong, Hong Kong, China

[4]Department of Building Environment and Energy Engineering, Department of Mechanical Engineering, The Hong Kong Polytechnic University, Hong Kong, China

Correspondence

Sau Chung Fu, Department of Mechanical Engineering, The University of Hong Kong, Hong Kong, China. Email: scfu@hku.hk

Acknowledgements

This work was supported by the Collaborative Research Fund (CRF) projects (no. C7025-16G and no. C1105-20GF)

Abstract

Head orientations directly determine movement directions of exhaled pathogen-laden droplets, while there is a lack of research about the effect of the infected person's head orientations on respiratory disease transmission during close contact. This work experimentally investigated the effect of different head orientations of an infected person (IP) on the bioaerosol deposition on a healthy person (HP) during close contact. Also, the effectiveness of PV flow in reducing bioaerosol deposition on the HP under the IP's different head orientations was investigated. Bacteriophage T3 was employed to represent viruses inside the cough-generated aerosols. The bioaerosol depositions on different locations of the HP's upper body (chest, shoulder, and neck) and face (chin, mucous membranes, cheek, and forehead) were characterized by a cultivation method. Results showed that the IP's different head orientations resulted in significantly different deposition density on the HP. PV flow could reduce the bioaerosol deposition remarkably for most cases investigated. The effectiveness of PV flow in reducing deposition on the HP was significantly affected by the IP's head orientations. Findings suggest that changing head orientations can be a control measure to reduce the bioaerosol deposition. Personalized ventilation can be a potential method to reduce the bioaerosol deposition on the HP.

Practical implications:

- Air distribution and human behaviours are important factors influencing the transmission of respiratory diseases.
- Changing head orientations and personalized ventilation can be good control measures to reduce bioaerosol deposition on healthy people.

- Deposition on mucous membranes in this work demonstrates the importance of protection (personalized ventilation, changing head orientations, masks, face shields, etc.) for the eyes, nose and mouth.
- The results provide useful information for the design of air distribution systems for better indoor environments.

Keywords: Head orientation, Personalized ventilation, Bioaerosol deposition, Close contact, Cough, Respiratory disease transmission

1 Introduction

Transmission of respiratory diseases, such as influenza, SARS, and COVID-19, has become a major concern in indoor environments since people spend more than 80% of their time indoors [1,2]. For example, the infection cases caused by COVID-19 have been reported in the hospital[3], schools[4], and restaurant[5] via the airborne route of virus transmission. Expiratory bioaerosols from expiratory activities, such as sneezing, coughing, talking and breathing, are the major source of respiratory disease transmission. During close contact, the expiratory bioaerosols from infected people can move directly to the exposed people and deposit on the environmental and human body surfaces. The deposited bioaerosols may be transferred to the mucous membranes by the route of fomite transmission, which results in a risk of infection. Studies revealed that, via the fomite route, the infection risk for SARS was around 50% in an aircraft cabin[6] and for influenza A was up to 93% in a residential bedroom[7]. In addition, 20%-40% of nosocomial infections were caused by the contaminated hands[8,9] and high-frequency touching surfaces[10]. Fomite transmission in these studies mainly focused on the pathogens deposited on the environmental surfaces. In fact, pathogens in expiratory aerosols also deposited on the human body surfaces and the touch frequency on the human body surfaces was higher than that on environmental surfaces[11]. Thus, in order to better evaluate the risk of

infection by the fomite transmission for deposition on human body surfaces, it is essential to investigate the pathogens deposited on the human body surfaces under different scenarios.

Expiratory aerosols deposited on the human body surface have been investigated in some studies. Liu et al.[12] indicated that 0.4% - 6.2% aerosols from breathing could deposit on the exposed person with an infected person at a distance from 0.5 m to 3 m. Xu et al.[13] indicated that lots of expiratory bioaerosols could deposit on the face and upper body parts of the exposed person facing an infected person at a distance from 0.5 m to 1.2 m. A recent study in a two-bed hospital ward[14] showed that 0.03% - 2.08% bioaerosol would deposit on the health care workers (HCW) under different ventilation systems. Different locations of the HCW resulted in the different deposition. Studies[15,16] in an aircraft cabin environment indicated that the passenger in the front of the cougher had the largest deposition rate compared to other passengers. These studies investigated the aerosol deposition on the human body while we found that these studies mainly focused on the expiratory aerosols released in a specific direction in each study.

In fact, during close contact, people like to turn left and right, and lower or raise their heads, besides looking forward or keeping upright[17]. In addition, studies showed that people would like to change the head/body movements and gesture dynamics to improve the perception of auditory speech[18] and express emotions[19]. The head orientation directly determines the direction of expelled pathogen-laden aerosols[20] and the expelled aerosols are the major contamination sources of respiratory disease transmission. Thus, it is also essential to know the impact of the infected people with different head orientations on the bioaerosol deposition on the exposed people. However, the related research is lacking on the effect of different infected person's head orientations on disease transmission.

In addition, aerosol deposition on the clothing and/or human skin could be resuspended due to motion caused by clothes removal, human physical activities, or body movements.

Aerosol resuspension is a probably secondary source of exposure for exposed persons in indoor environments [21]. Nikfar et al. [22] suggested that the resuspension of respiratory aerosols from surfaces was highly related to droplet size, initial droplet velocity and surface wettability. Licina et al. [23] indicated that resuspension of size-resolved airborne particles from clothing is a function of motion type, intensity, dust loadings and activity duration. Gomes et al. [24] reported that particle resuspension was mainly affected by air swirl intensity. By comparing resuspension of aerosols with diameters of 3, 5, 10 μm from clothing surfaces, larger aerosols increased the likelihood of resuspension. Different physical activity levels and clothing's weave patterns resulted in different resuspension rates [25,26]. A chamber study showed that walking, sitting, upper body movements or interactions between clothing and human skin could cause different degrees of resuspension [27]. These studies provided useful information for aerosol resuspension. Besides the factors mentioned in these studies, the resuspended aerosols highly depended on their initial concentrations on the clothing and human skins. However, the information on aerosol concentration or distribution on the clothing/human skins is still lacking.

Personalized ventilation (PV) has been suggested as a potential method to reduce respiratory disease transmission in indoor environments. Usually, PV is utilized together with total volume ventilation, such as displacement ventilation (DV), underfloor air distribution (UFAD) systems, mixing ventilation (MV), or chilled ceilings [28-30]. The supplied clean air by PV can be from outdoor conditioned air or recirculated room air. If recirculated room air is used, a high-efficiency particulate air (HEPA) filter would be installed in the air duct of the PV system to ensure the cleanliness of the supplied air by PV. For example, a previous study reported a HEPA filter with an efficiency of 99.5% was used in PV system [31]. Then, PV can provide clean air to the users as close as possible to achieve better indoor air quality [32]. The effectiveness of PV in reducing contamination under different scenarios have been investigated. Pantelic et al.[33] showed that PV flow could reduce the intake fraction of airborne aerosols between 41% and

99% considering the distance and orientations of the cough release relative to the exposed person. Li et al.[29] showed that, when the PV was used by a healthy person, exposure of the healthy person to airborne aerosols could be significantly reduced no matter whether the infected person used PV or not. Lipczynska et al.[30] indicated the system of PV combined with a chilled ceiling can substantially reduce the concentration of infectious air at workstations and also meet the requirement of thermal comfort. Numerical studies[28,34] investigated the protection of PV with different terminals and flow rates on the users and results indicated that PV performance has a high relationship with the terminals and flow rates. These studies demonstrated that PV can be a potential method to reduce the concentration of airborne aerosols in the inhalation zone.

We can find that, firstly, these aforementioned studies mainly focused on the effectiveness of PV on the reduction of airborne aerosols. As discussed above, besides the inhalation of airborne aerosols, pathogen-laden expiratory aerosols also deposit on surfaces, as the source of fomite transmission, and pose a high risk of infection. But limited studies investigated the performance of PV flow in reducing the deposition of pathogen-laden droplets on the PV users. Assaad et al.[35] showed that, for aerosols with a low initial velocity of 1 m/s, increasing the flow rate of PV flow could result in a higher deposition rate of particles on the PV user and nearby surfaces. Different from the particles with a low initial velocity, cough-generated aerosols have a large initial velocity (11.7 m/s)[36] and can easily impact nearby surfaces. Xu et al.[13] indicated that PV could reduce the bioaerosol deposition of cough-generated aerosols on the healthy person when the infected person was located at a distance from 0.5 m to 1.2 m. The different results indicated that more studies about the performance of PV flow in bioaerosol deposition need to be further investigated. Secondly, the different head orientations of the infected person may also play an important role in the performance of PV flow. So far, it is still unknown the effect of the IP's head orientations on the performance of PV flow.

Thus, the objective of this work was to investigate the performance of the infected person's head orientation and the effectiveness of PV flow in reducing the bioaerosol deposition on the PV user. Bacteriophage T3 was used to represent the virus from the coughing activities. An infected person (thermal manikin) released the cough-generated aerosols with seven head orientations. The concentration of bacteriophage on the surfaces of the PV user were characterized by the cultivation method.

2 Experimental Instruments and Methods

2.1 Bioaerosol generation

Bacteriophage T3 (ATCC 11303-B3) and the host *Escherichia coli* (ATCC 11303) with a safety level of one was used to represent the viral pathogens into expiratory aerosols. After propagation, harvest, and centrifugation, a high titre bacteriophage solution was prepared in advance and stored at 4 ^{o}C. The detailed protocol can be found in supporting information. Then some titration solution was added to 200 mL simulated saliva solution, and the initial concentration of the bacteriophage in the saliva solution was 10^6 PFU/ml, which was measured by serial dilution and the soft-agar overlay technique. Simulated saliva solution was made by dissolving 76 g of glycerin and 12 g of salt (NaCl) in 1 liter of sterilized distilled water[15]. A custom-built cough generator was used to generate the cough aerosols using the prepared saliva solution with bacteriophage viruses. The cough generator had been used in previous studies [15,37,38]. The size distribution and initial velocity were measured by interferometric Mie imaging (IMI) and a particle imaging velocimetry (PIV) technique, respectively. The characteristics of generated aerosols were shown in Fig. 1S in the supporting information. The aerosols released from the cough generator had a peak size range of 10–20 μm, which was similar to that of a real cough. The velocity of released aerosols was around 12 m/s, similar to the average

coughing velocity of 11.7 m/s [36]. The air-atomizing nozzle of the aerosol generator was positioned at the mouth of a thermal manikin, which was called the infected person (IP).

2.2 Experimental setup

The experiment was performed in a chamber having a dimension of 4.0 m (length) × 2.6 m (width) × 2.3 m (height), as shown in Fig. 1. During the experiment, the temperature and relative humidity were controlled at 23 ± 1 ^{o}C and 65 ± 5%, respectively. An air conditioner unit was used to control the indoor temperature. The air recirculation was around 14 times per hour, which was measured by a capture hood (Model 8380, TSI, USA) with a resolution of 1 m^3/h. Two seated male-shaped thermal manikins[13] were used to simulate a healthy person (HP) and the IP. The sitting height and clothing insulation were 1.4 m and 0. 46 clo, respectively. The heat release rate for each manikin was 70 W for moderate office work[39]. A PV system connecting to another chamber supplied clean air directly to the HP. The PV terminal was towards the HP's face, as shown in Fig. 1. The diameter of the PV terminal was 0. 108 m. A honeycomb flow straightener (holes diameter of 3.5 mm, thickness of 20 mm) was inserted into the PV outlet to reduce the turbulence. In addition, a high-efficiency particulate air (HEPA) filter (H13 filter, PM0.3, 99.97%) was installed in the air duct of the PV system to ensure that PV provided clean airflow. The flow rate of PV in this work was set 16 L/s. The PV velocity and turbulence intensity in the inhalation zone of the HP were around 1.2 m/s and 7% respectively, which was measured by an omni-directional anemometer (Swema 03) with a velocity range of 0.05-3.0 m/s and an accuracy error of ± 4%. The exhaust only worked when PV was used.

A recent study indicated that, during close contact, people probably turn right or left, raise or lower their heads and the angle between 0^{o} and 30^{o} [17]. In this study, five head orientations in the vertical direction and two orientations in the horizontal direction of the IP were investigated. When the IP's head horizontally pointed the HP, it was labelled H0; when the IP lowered down

the head at angles of 12° and 24°, it was labelled L12 and L24, respectively; when the IP raised the head at angles of 12° and 24°, it was labelled H12 and H24, respectively; when the IP turned the head in the right direction at angles of 12° and 24°, it was labelled R12 and R24, respectively. The horizontal distance between the IP and HP in each case was kept at 0.66 m to simulate a short contact distance[17] since the study indicated that the average distance between two people was 0.66 m. To simplify the experimental setup, different head orientations of the IP was realized by adjusting the angle of the nozzle of the cough generator, as shown in Fig. 2. For example, at H24, the IP raised the head at 24°. It meant the angle between the nozzle of the cough generator and the horizontal line was 24°.

During the experiment, three coughs were generated and each one lasted one second with an interval of 30 seconds from the IP. With the IP's head at different orientations, the bioaerosol deposition on the HP with and without PV was measured. After each measurement, two ultraviolet light ozone generators worked for 30 minutes for sterilization. After that, enough time was given for ventilation to clean the chamber before the next measurement. Simultaneously, an ozone monitor was used to check ozone concentration during the process to ensure there was no influence on the next measurement. To check the effect of sterilization, a control experiment was performed after sterilization and ventilation. The clean silicone face mask and silicone samples were attached to the HP's face and upper body, respectively. No cough was released. Then, the same collection and cultivation methods as the experimental process were used. No virus was detected. The control experiment showed that sterilization was effective.

2.3 Measurement of bioaerosol deposition on the HP manikin

The number of viable viruses deposited on the HP's face and upper body was measured. For the HP's face, a 3-D silicone mask with a plastic support [13] was attached to the HP's face before the experiment. The face was divided into four parts: forehead, cheek and chin and

mucous membranes, as shown in Fig. 3. For the upper body part, the viable viruses deposited on the chest, neck and shoulders were measured. Silicone samples for the chest (25 cm ×14 cm), shoulders (5 cm ×14 cm × 4 cm) and neck (5 cm × 38 cm) of the HP were positioned for sampling before the experiment (Fig. 3). The silicone masks and samples were cleaned with medical grade-alcohol solution and dried for five minutes before experiments. After the experiment, the mask and silicone samples from the HP were collected, Sterilized cotton buds were used to collect the viruses by a swabbing method. The cotton buds for each tested area were put in 30 ml of saline solution. After vibration, 1 ml saline solution with viruses and 0.3 ml *E. coli* solution was mixed for 15 min. After that, the soft-agar overlay technique [38] was used and the plates were put in an incubator at 37 ºC for 6 h, then the plaque forming unit (PFU) could be obtained from each place.

The possible potential interactions between silicone material and deposited bioaerosols was checked. Compared to that of the Petri dish, the mask and silicone samples did not influence the virus viability. The test process can be found in the supporting information. To improve the accuracy of the results by the cultivation method, each case was repeated three times. The temperature and relative humidity during the experiment was kept stable. The protocol of the cultivation method was carefully followed.

Mucous membranes consist of one or more layers of epithelial cells overlying a layer of loose connective tissue. The thin epidermal layers of mucosal surfaces are less protective. Usually, the mucosal region on the face was the eyes, nostril/nose, and mouth of exposed persons. In this work, the mucous membranes include the part of eyes, nose and mouth noted by red curves in Fig. 3. The area of mucous membranes investigated in this work was in line with that of previous studies [7,40,41]. For the part of the nose, since there were no nostrils in the mask used, the mucous membranes of the nose part did not include the inside of the nose while included the part under the nose and the cross section of the nose. The sampling on the mucous

membranes was the same as that on the face using the swabbing method. The direct projection of expiratory droplets on the mucous membranes is called the droplet route, which is a possible exposure pathway for infection. To quantify the exposure caused by the droplet route, mucous membranes were as a whole area and deposition on the membranes was investigated together.

The deposition density on each part was calculated using the following equation (1):

$$Deposition\ density\ = \frac{(Number\ deposition)_{sampling}}{A_{sampling}} \quad (1)$$

where $A_{sampling}$ (cm^2) was the surface area of the silicone sheets for sampling on each part of the HP. The $(Number\ deposition)_{sampling}$ (PFU) was the total number of deposited viable viruses on the silicone sheets of each part. The unit of the *Deposition density* was PFU/cm^2.

2.4 Visualization experiment

The interaction between the PV flow and the cough jet from different head orientations was observed. The experiment was arranged as shown in Fig. 2S, Two LED lights were used as the light source. A camera with five frames per second was used to record the interaction. Due to 'cold light' for LED, the temperature around the HP and IP was maintained before and after the LED was turned on. We thought that the LED light had little influence on the interaction between the motion of the cough jet and PV flow.

3 Results

This work investigated bioaerosol deposition on the HP exposed to cough aerosols from the IP with different head orientations. Meanwhile, the performance of PV flow in reducing the bioaerosol deposition on the HP under different IP's head orientations was studied.

3.1 Effect of head orientations on deposition density under cases without PV

When the head orientation was at H0, the cough jet was released horizontally and reached the HP around 0.4-0.6 s. It was mainly around the HP's face part, as shown in Fig. 4. At 0.6 –

1.4 s, the HP's face was covered by the cough jet. At H12 (Fig. 5(a)), the cough jet slanted upward and mainly concentrated on the forehead. When the cough jet impinged on the face, the cough jet spread along the face. Part of the cough jet moved upward along the face and part of the cough jet moved downward along the face, as shown in Fig. 5(a) of the motion of the cough jet at t = 1.0 s and 1.2 s. At H24, the cough jet slanted upward further and was above the forehead. The cough jet almost avoided the face and upper body part (Fig. 3S). Under L12 (Fig. 4S) and L24 (Fig. 5S) cases, the cough jet mainly impinged on the HP's neck and chest, respectively.

Aerosols generated from the cough generator was poly-dispersed and the size distribution was similar to a real cough. The peak size range was around 10-20 μm, as shown in Fig. 1S. A numerical study by Wei et al. [42] indicated that expiratory aerosols with diameters of 10, 50, 100 μm followed the cough jet within a distance of 0.7 m from the release point. In addition, experimental studies by Wang et al. [37] also showed that airborne and large aerosols could directly impinge on the front flat surface within the distance of 1.1 m. In this work, the short horizontal distance (0.66 m) between the HP and the cough generator meant that the aerosols generated could follow the cough jet and impinged on the HP under different head orientations.

Fig. 6(a) shows the deposition density on the HP when the IP's head orientations were from L24 to H24. The deposition density of bioaerosol on the HP was largely affected by the IP's head orientations. For the HP's face part, the deposition density on the chin, mucous membranes, cheek, and forehead was significantly different due to different head orientations. For example, the deposition density on the forehead was increased from L24 to H12 and then reduced to L24. Compared with the highest deposition density on the forehead at H12, head orientations of the IP resulted in a reduction between 85% and 99%. The highest deposition density on the chin was at L12, on the mucous membranes and cheek was at H0, and on the forehead was at H12.

Special attention should be paid to the mucous membranes (shown in Fig. 3(b)) since the mucous membrane barriers are less effective than those of intact skin [43]. Deposition density first increased from L24 to H0 then decreased to H24. When the head orientation was from L24 to H24, the cough jet deviated from the HP's mouth at L24 case, gradually was close to the mouth area at L12. Then, the cough jet mainly focused on the face at H0 and density reached the highest at H0. At H12, the cough jet deviated the HP's mouth again, but it still covered the eyes and nose (Fig. 5 (a)). At H24, the cough jet was far away from the area of the eyes. So, the density was reduced from the highest at H0 to L24. Compared with the maximum density at H0, head orientations resulted in a reduction between 64% and 99%.

Similarly, the IP's head orientations resulted in a large difference in deposition density on the upper body part (chest, shoulder, and neck), as shown in Fig. 6(a). For example, deposition density on the chest was reduced dramatically when the head was from L24 to H24. The cough jet mainly focused on the chest part at L24, when the head orientation was from L24 to H24, the cough jet was gradually far away from the chest area. Compared with the highest value at L24, the deposition density on the chest could be reduced by 60%-99%. The highest deposition density on the chest was at L24, on the shoulder and neck was at L12.

Fig. 6 (b) shows the deposition density on the HP when the IP's head was from H0 to R24 in the right direction. At R12 and R24 cases, the cough jet deviated from the HP's face part. Deposition density on the chin, mucous membranes, cheek, and forehead was decreased dramatically when the head was from H0 to R12 and R24. Especially, at R24 case, there were only few bacteriophages on the forehead detected on the face. For the upper body part, Deposition density on the shoulder was increased from H0 to R12 and then decreased to R24 since, at R12, the cough jet was above the shoulder, some large aerosols deposited on the right shoulder. At R24, the cough jet was away from the shoulder. So, the deposition density was reduced.

3.2 Effect of PV

The deposition density on the HP's face and body influenced by PV under different head orientations was investigated. When the IP's head orientation was from L24 to H24 (L24, L12, H0, H12, and H24), for the face (the chin, mucous membranes, cheek, and forehead) part, PV flow could reduce the deposition density for all cases except at L24, as shown in Fig. 7. For example, at H12, the reduction of deposition density on the chin, mucous membranes, cheek and forehead was between 89% to 98% compared to that without PV. Fig. 5(b) shows the interaction between the cough jet and PV flow at H12. The cough jet was blown upward by PV flow and was above the HP's forehead, which was quite different from that without PV (Fig. 5(a)) where part of the cough jet could move downward along the face part. Similarly, the interaction between the cough jet and PV flow around the HP at H24 was shown in Fig. 6S.

Fig. 8 shows that the deposition density on the upper body part (the chest, shoulder and neck) was influenced by PV flow when the head orientations were from L24 to H24. PV flow could significantly reduce the deposition density on the chest, shoulder and neck at L12, H0, H12 and H24. For example, the reduction on the neck was between 34% and 99% compared to each case without PV.

Differently, at L24, though PV flow reduced the deposition density on the chin, forehead, and chest, PV flow slightly increased the deposition density on the mucous membranes, check, and shoulder. The possible reason was that when the cough jet encountered the PV flow at L24, the core area of the PV flow diluted part of the cough jet while some aerosols were entrained by the periphery of PV flow. It implies that PV is not suitable to be used when the contamination source is quite close to the PV terminal. To better understand this result, numerical simulation can be used to explore the reason behind it in future work.

When the head orientation was from H0 to R12 in the right direction, at R12, PV flow moderately reduced the deposition density on the face (chin, mucous membranes, cheek and forehead) in Fig. 7 and the chest in Fig. 8. The reduction was smaller than that of other head orientations. The possible reason was that, at R12, the cough jet tilted in the right direction while the PV flow focused on the HP's face part. The PV flow did not directly interact with the cough jet. However, the PV flow at R12 increased the deposition on the shoulder as shown in Fig. 8 (b), possibly because that the periphery of PV flow entrained some aerosols around the right shoulder. The deposition density on the shoulder was increased by PV flow.

By comparing the results, it can be found that, even though PV flow was pointing to the face area, the reduction in the chin, mucous membranes, cheek, and forehead of the face caused by PV differed significantly. For example, at H0, the reduction on the chin, mucous membranes, cheek and forehead was 95%, 74%, 84% and 64% compared to each case without PV, respectively. Simultaneously, head orientations resulted in a different performance of PV in reducing the deposition density on the same surfaces. For instance, reduction caused by PV flow on the mucous membranes was from -192% to 89% when the head orientation was from L24 to H24.

Based on the measurement from a previous study [37], when the distance between the cough generator and a front vertical surface was 0.5 m, the velocity of cough-generated aerosols reaching the vertical surface was around 1.4 m/s. Similarly, when the distance was 0.8 m, the corresponding velocity was 1 m/s. In this work, the horizontal distance between the cough generator and the HP was 0.66 m. The velocity of aerosols when reaching the HP's face was estimated around 1.2 m/s. The PV velocity around the inhalation zone was also at around 1.2 m/s. A previous study showed that the air motion caused by the thermal plume around the breathing zone was about 0.17 m/s [44]. Though the upward air motion caused by thermal plume could slightly increase the upward air motion caused by PV and help to drive the cough jet

upward, the small velocity of air motion caused by thermal plume probably had a marginal effect on the deposition influenced by PV.

4 Discussion

This work mainly investigated the effect of the IP's head orientations on the aerosol deposition on the HP and the performance of PV in reducing deposition under the IP's different head orientations. The findings demonstrated that different head orientations resulted in significantly different deposition density on the HP. In addition, the effectiveness of PV in reducing deposition density was highly related to the IP's head orientations.

The IP's different head orientations led to a substantial difference in deposition density on the HP in this work. Head orientations determined the movement direction of the cough jet and the following impingement point on the HP. The cough jet impingement points matched well with the high concentration parts of the HP. The significantly different deposition density caused by the IP's head orientations in this work suggests that head orientation can be a good control measure to reduce aerosol deposition on the HP. Compared to H0 case, the low deposition density at cases of R24, R12 and H24 implies that, during close contact, it is good to turn the head away when people are coughing or sneezing. In another way, it is quite important for the HP to avoid directly exposing the cough or sneezing jet.

PV flow significantly reduces the deposition density on the HP for most cases while it also increased the deposition density on the HP at L24 and R12 in this work. PV flow mainly has two functions for the aerosols. One is that PV sends the clean air to the users and dilutes the expiratory aerosols; One is that the PV flow entrains aerosols and increases the exposure to expiratory aerosols. The performance of PV in different cases mainly depends on the balance of the advantage and disadvantage. Thus, in order to better understand the protection of PV and

promote the application of PV in the control of respiratory disease transmission, more studies under different complex scenarios should be investigated.

Some studies[13,31,45] showed that PV flow can reduce exposure to airborne aerosols. This work showed that PV can also reduce the deposition density on the HP. Combined with findings in this work and previous studies, PV can be a potential method to reduce the deposition density and exposure to airborne aerosols simultaneously.

The effectiveness of PV flow in reducing deposition was significantly influenced by different head orientations in this work. The upward PV airflow formed an air curtain in the front of the HP's face. The cough jet with different movement directions resulted in different interactions between the PV and the cough jet around the HP. The different interaction around the HP in this work implies that the IP's head orientations may also result in different effectiveness of PV in reducing inhalation of airborne aerosols. For example, Alsaad et al.[46] indicated that PV flow has different effectiveness in reducing the contaminants from different sources (e.g., the exhalation of the IP, groins of the IP, and trash bins). Thus, further studies should be performed to investigate the impact of IP's head orientation on the PV performance in reducing the exposure to airborne aerosols.

In addition, the same cough generator was also used in previous studies. Wang et al. [38] studied the flow dynamics of the cough jet under the effect of a downward gasper jet. They found that the cough jet including aerosols and cough airflow was bent downward by the gasper jet. Both airborne and large aerosols deposited at a lower position of the front surface compared to that without the gasper jet. In addition, both the concentration of airborne and large aerosols for deposition was reduced. Increased velocity of gasper jet from 0.7 m/s to 2.5 m/s resulted in an exponentially decreased deposition on the front surface. Xu et al. [13] found that the upward PV flow could significantly reduce the inhalation and deposition of bioaerosol generated from

the cough generator. The increased PV velocity from 0.75m/s to 1.6 m/s further reduced inhalation and deposition on the most parts investigated on the HP. Differently, this work mainly studied the performance of PV flow at one velocity in reducing bioaerosol deposition under different the IP's head orientations. As the above analysis, changing PV velocity would result in different protection efficiency of PV. The fixed PV velocity is a limitation of this work, which suggests that the investigation of PV at different flow rates in the future can further provide useful information for better ventilation design and individual protection.

The most important advantage of PV is to supply clean air to the users as close as possible to improve the indoor air quality. This work mainly focused on the protection of PV, but the high velocity of PV airflow around the face might cause eye irritation or draught risk for the users concurrently, which possibly resulted in an adverse effect on the utilization of PV. Previous studies showed that in warm environments PV could effectively improve the thermal comfort [47,48] and the ambient temperature could be 4-5 ºC higher than the temperature recommended by current standards [49]. Dalewski et al. [50] indicated that, when the ambient temperature was 26 ºC and 29 ºC, most of the subjects preferred the personalized air velocity in the range 1.2-1.5 m/s and 1.5-1.7 m/s, respectively. Similarly, Schiavon et al. [51] reported that, when the local velocity was at 0.9 m/s and 1.5 m/s, neutral thermal sensation votes could be obtained with indoor temperatures of 26 ºC and 29 ºC respectively. Lipczynska et al. [30] suggested that, when the indoor temperature was 28 ºC, PV velocity at 1.0-1.3 m/s resulted in an equivalent temperate of 18 ºC at the face surface and people perceived more refreshing. In this work, the ambient temperature was around 23ºC. PV flow might result in discomfort for the HP. Thermal comfort is highly related to the indoor temperature, relative humidity, air motion, human clothing, and activities level. To enhance the application of PV, further work should systematically investigate the performance of PV in indoor air quality (IAQ), thermal comfort, and energy savings under different dynamic operating situations. In addition, it is

essential to explore the optimization of the PV design based on the reasonable balance between IAQ, thermal comfort and energy saving or particular focus (e.g., protection).

In this work, the position of PV was fixed at the center of the HP as shown in Fig. 1 and the protection of PV was investigated under this setting. The fixed position of PV is a limitation of this study. In reality, PV position is possibly altered, which is also an advantage of PV, that is individual control. For example, PV might be put on the side rather than the center of the users. Besides PV position, users can also adjust the air velocity, direction, and operation based on their preferences. The protection of PV in this work implies that, in different situations, PV likely still protects the users while the protection efficiency needs further investigation based on specific setups.

The number of deposited bacteriophages on the HP's face and body in this work, as a contamination source for the fomite transmission, will pose a threat for disease transmission [6,52]. The deposited pathogens on the HP can be transferred from hands to mucous membranes due to fomite transmission. Deposition density in this work can provide boundary conditions for further work to investigate the risk of infection caused by fomite transmission or the droplet route. Simultaneously, the deposition on the mucous membranes in this work indicates the importance of protection, such as masks and face shields, for the mucous membranes of eyes, nose and mouth. Furthermore, resuspension from the clothing/human skins is a probably secondary route of exposure of a healthy person or other people co-sharing the space. The deposition on the HP in this work provides the boundary conditions of virus loading for resuspension modelling proposed in previous studies.

The collection method of swabbing used in this work was as a standard method for collection and was widely accepted for surface sampling method [53-55]. Previous studies [56-58] suggested the swabbing efficiency was around 41%-58%, which was highly related to surface

material, pathogen species and touch force. The same material of silicone was used for the face and body sampling to avoid the different swabbing efficiency caused by different surface materials. The standard swabbing procedures were followed in this work to ensure the consistent swabbing efficiency. The swabbing efficiency might lead to an underestimation of the bioaerosol deposition on the HP.

The cultivation method used in this work was mainly to determine viable and culturable organisms. Differently, qPCR (quantitative polymerase chain reaction) was used to detect and quantify nucleic acids. The combined utilization of cultivation methods and qPCR in further studies could provide more information to understand the deposited aerosols.

There are some limitations in this work. The deposition of bacteriophage was collected from the surface of the silicone material, which was different from the real surfaces of the face and clothes. This work did not consider the viscosity of the mucous membranes. The liquid/sticky mucous membranes are possibly easier to capture the aerosols and increase the aerosol deposition [59]. In order to improve the accuracy of measurements, a more realistic face mask is needed for further studies. Due to the limit of the air conditioner unit in the test chamber, the airflow rate of 14 h^{-1} was used in this work, which was higher than that in offices [34] and residential buildings [60,61]. Besides, the deposition on the eyes (part of the mucous membranes) may be influenced by the eyelashes and blinking of the eyes of the HP. Therefore, future work should further investigate the impact of eyelashes and blinking of eyes on the deposition of cough aerosols on the eyes.

Conclusions

This work investigated the effect of head orientations and PV flow on bioaerosol deposition. The head orientations of the IP played a significant role in the bioaerosol deposition of the HP. Changing the head orientations could result in significantly different bioaerosol

deposition on the HP. PV flow was able to reduce the bioaerosol deposition effectively for the majority of the cases. But, at R12 and L24 cases, PV flow increased the bioaerosol deposition. The effectiveness of PV in reducing bioaerosol deposition is highly related to the IP's head orientations. This study suggested that changing head orientation to avoid direct exposure to a cough jet is a possible way to reduce bioaerosol deposition. PV can be a potential method to reduce bioaerosol deposition. The performance of PV in reducing deposition depended on the balance of advantage and disadvantage between PV flow and aerosols. Bioaerosol deposition on the HP in this work provides useful information about boundary conditions for the modelling of fomite transmission and resuspension route to further improve the accurate of the infection risk assessment. In order to better promote the applications of PV, systematic studies about thermal comfort, indoor air quality, and energy saving for PV under realistic situations should be conducted.

Declaration of Conflicting Interests

No conflict of interest declared.

References

1. Benner Jr BA, Gordon GE, Wise SA. Mobile sources of atmospheric polycyclic aromatic hydrocarbons: a roadway tunnel study. *Environ Sci Technol.* 1989;23(10):1269-1278.

2. Robinson J, Nelson W. National human activity pattern survey data base. *USEPA, Research Triangle Park, NC.* 1995.

3. Lednicky JA, Lauzard M, Fan ZH, Julta A, Tilly TB, Gangwar M, Usmani M, Shankar SN, Mohamed K, Eiguren-Fernandez A. Viable SARS-CoV-2 in the air of a hospital room with COVID-19 patients. *Int J Infect Dis.* 2020;100:476-482.

4. Lessler J, Grabowski MK, Grantz KH, Badillo-Goicoechea E, Metcalf CJE, Lupton-Smith C, Azman AS, Stuart EA. Household COVID-19 risk and in-person schooling. *Science.* 2021;372(6546):1092-1097.

5. Li Y, Qian H, Hang J, Chen X, Cheng P, Ling H, Wang S, Liang P, Li J, Xiao S. Probable airborne transmission of SARS-CoV-2 in a poorly ventilated restaurant. *Build Environ.* 2021;196:107788.

6. Lei H, Li Y, Xiao S, Lin CH, Norris SL, Wei D, Hu Z, Ji S. Routes of transmission of influenza A H1N1, SARS CoV, and norovirus in air cabin: Comparative analyses. *Indoor Air.* 2018;28(3):394-403.

7. Nicas M, Jones RM. Relative contributions of four exposure pathways to influenza infection risk. *Risk Anal: An International Journal.* 2009;29(9):1292-1303.

8. Weber DJ, Rutala WA, Miller MB, Huslage K, Sickbert-Bennett E. Role of hospital surfaces in the transmission of emerging health care-associated pathogens: norovirus, Clostridium difficile, and Acinetobacter species. *Am J Infect Control.* 2010;38(5):S25-S33.

9. Kundrapu S, Sunkesula V, Jury LA, Sitzlar BM, Donskey CJ. Daily disinfection of high-touch surfaces in isolation rooms to reduce contamination of healthcare workers' hands. *Infect Control Hosp Epidemiol.* 2012;33(10):1039-1042.

10. Otter JA, Yezli S, French GL. The role of contaminated surfaces in the transmission of nosocomial pathogens. In: *Use of Biocidal Surfaces for Reduction of Healthcare Acquired Infections.* Springer; 2014:27-58.

11. Zhang N, Li Y, Huang H. Surface touch and its network growth in a graduate student office. *Indoor Air.* 2018;28(6):963-972.

12. Liu L, Li Y, Nielsen PV, Wei J, Jensen RL. Short-range airborne transmission of expiratory droplets between two people. *Indoor Air.* 2017;27(2):452-462.

13. Xu J, Wang C, Fu S, Chan K, Chao CY. Short-range Bioaerosol Deposition and Inhalation of Cough Droplets and Performance of Personalized Ventilation. *Aerosol Sci Technol.* 2021;55(4):474-485.

14. Liu Z, Wang L, Rong R, Fu S, Cao G, Hao C. Full-scale experimental and numerical study of bioaerosol characteristics against cross-infection in a two-bed hospital ward. *Build Environ.* 2020;186:107373.

15. Sze To G, Wan M, Chao C, Fang L, Melikov A. Experimental study of dispersion and deposition of expiratory aerosols in aircraft cabins and impact on infectious disease transmission. *Aerosol Sci Technol.* 2009;43(5):466-485.

16. Wan MP, Sze To GN, Chao CYH, Fang L, Melikov A. Modeling the fate of expiratory aerosols and the associated infection risk in an aircraft cabin environment. *Aerosol Sci Technol.* 2009;43(4):322-343.

17. Zhang N, Tang JW, Li Y. Human behavior during close contact in a graduate student office. *Indoor Air.* 2019;29(4):577-590.

18. Munhall KG, Jones JA, Callan DE, Kuratate T, Vatikiotis-Bateson E. Visual prosody and speech intelligibility: Head movement improves auditory speech perception. *Psychol Sci.* 2004;15(2):133-137.

19. Castellano G, Villalba SD, Camurri A. Recognising human emotions from body movement and gesture dynamics. Paper presented at: *International Conference on Affective Computing and Intelligent Interaction* 2007:71-82.

20. Ai Z, Melikov AK. Airborne spread of expiratory droplet nuclei between the occupants of indoor environments: a review. *Indoor Air.* 2018;28(4):500-524.

21. Qian J, Peccia J, Ferro AR. Walking-induced particle resuspension in indoor environments. *Atmos Environ*. 2014;89:464-481.

22. Nikfar M, Paul R, Islam K, Razizadeh M, Jagota A, Liu Y. Respiratory droplet resuspension near surfaces: Modeling and analysis. *J Appl Phys.* 2021;130(2):024702.

23. Licina D, Nazaroff W. Clothing as a transport vector for airborne particles: chamber study. *Indoor Air.* 2018;28(3):404-414.

24. Gomes C, Freihaut J, Bahnfleth W. Resuspension of allergen-containing particles under mechanical and aerodynamic disturbances from human walking. *Atmos Environ*. 2007;41(25):5257-5270.

25. McDonagh A, Byrne M. A study of the size distribution of aerosol particles resuspended from clothing surfaces. *J Aerosol Sci*. 2014;75:94-103.

26. McDonagh A, Byrne M. The influence of human physical activity and contaminated clothing type on particle resuspension. *J Environ Radioact.* 2014;127:119-126.

27. Bhangar S, Adams RI, Pasut W, Huffman JA, Arens EA, Taylor JW, Bruns TD, Nazaroff WW. Chamber bioaerosol study: human emissions of size-resolved fluorescent biological aerosol particles. *Indoor Air*. 2016;26(2):193-206.

28. Shen C, Gao N, Wang T. CFD study on the transmission of indoor pollutants under personalized ventilation. *Build Environ.* 2013;63:69-78.

29. Li X, Niu J, Gao N. Co-occupant's exposure to exhaled pollutants with two types of personalized ventilation strategies under mixing and displacement ventilation systems. *Indoor Air.* 2013;23(2):162-171.

30. Lipczynska A, Kaczmarczyk J, Melikov AK. Thermal environment and air quality in office with personalized ventilation combined with chilled ceiling. *Build Environ.* 2015;92:603-614.

31. Xu C, Wei X, Liu L, et al. Effects of personalized ventilation interventions on airborne infection risk and transmission between occupants. *Build Environ*. 2020:107008.

32. Melikov AK. Personalized ventilation. *Indoor Air.* 2004;14:157-167.

33. Pantelic J, Tham KW, Licina D. Effectiveness of a personalized ventilation system in reducing personal exposure against directly released simulated cough droplets. *Indoor Air.* 2015;25(6):683-693.

34. He Q, Niu J, Gao N, Zhu T, Wu J. CFD study of exhaled droplet transmission between occupants under different ventilation strategies in a typical office room. *Build Environ.* 2011;46(2):397-408.

35. Al Assaad D, Habchi C, Ghali K, Ghaddar N. Effectiveness of intermittent personalized ventilation in protecting occupant from indoor particles. *Build Environ.* 2018;128:22-32.

36. Chao CYH, Wan MP, Morawska L, Johnson GR, Ristovki ZD, Hargreaves M, Mengersen K, Corbett S, Li Y, Xie X, Katoshevski D. Characterization of expiration air jets and droplet size distributions immediately at the mouth opening. *J Aerosol Sci.* 2009;40(2):122-133.

37. Wang CT, Fu SC, Chao CYH. Short-range bioaerosol deposition and recovery of viable viruses and bacteria on surfaces from a cough and implications for respiratory disease transmission. *Aerosol Sci Technol.* 2021;55(2):215-230.

38. Wang C, Xu J, Fu SC, Chan KC, Chao CY. Respiratory bioaerosol deposition from a cough and recovery of viable viruses on nearby seats in a cabin environment. *Indoor Air.* 2021;31(6):1913-1925.

39. Handbook A. ASHRAE handbook–fundamentals. *Atlanta, GA.* 2009.

40. Tang JW, Gao CX, Cowling BJ, et al. Absence of detectable influenza RNA transmitted via aerosol during various human respiratory activities–experiments from Singapore and Hong Kong. PLoS One. 2014;9(9): e107338.

41. Chen W, Zhang N, Wei J, Yen H-L, Li Y. Short-range airborne route dominates exposure of respiratory infection during close contact. *Build Environ*. 2020;176:106859.

42. Wei J, Li Y. Enhanced spread of expiratory droplets by turbulence in a cough jet. *Build Environ.* 2015;93:86-96.

43. Hadrup N, Sharma AK, Loeschner K. Toxicity of silver ions, metallic silver, and silver nanoparticle materials after in vivo dermal and mucosal surface exposure: A review. *Regul Toxicol Pharmacol.* 2018;98:257-267.

44. Licina D, Pantelic J, Melikov A, Sekhar C, Tham KW. Experimental investigation of the human convective boundary layer in a quiescent indoor environment. *Build Environ*. 2014;75:79-91.

45. Xu J, Fu S, Chao CY. Performance of airflow distance from personalized ventilation on personal exposure to airborne droplets from different orientations. *Indoor Built Environ.* 2020:1420326X20951245.

46. Alsaad H, Voelker C. Could the ductless personalized ventilation be an alternative to the regular ducted personalized ventilation? *Indoor Air.* 2020;31(1):99-111.

47. Yang J, Melikov AK, Fanger PO, Li X, Yan Q. Impact of personalized ventilation on human response: comparison between constant and fluctuating airflows under warm condition. Paper presented at: *Proceedings of Roomvent*. 2002:305-308.

48. Zeng Q, Kaczmarczyk J, Melikov A, Fanger PO. Perceived air quality and thermal sensation with personalized ventilation system. Paper presented at: *Proceedings of roomvent.* 2002:61-64.

49. Veselý M, Zeiler W. Personalized conditioning and its impact on thermal comfort and energy performance – A review. *Renew Sust Energ Rev*. 2014;34:401-408.

50. Dalewski M, Melikov AK, Vesely M. Performance of ductless personalized ventilation in conjunction with displacement ventilation: Physical environment and human response. *Build Environ*. 2014;81:354-364.

51. Schiavon S, Yang B, Donner Y, Chang VC, Nazaroff WW. Thermal comfort, perceived air quality, and cognitive performance when personally controlled air movement is used by tropically acclimatized persons. *Indoor Air*. 2017;27(3):690-702.

52. Lei H, Li Y, Xiao S, Yang X, Lin CH, Norris SL, Wei D, Hu Z, Ji S. Logistic growth of a surface contamination network and its role in disease spread. *Sci Rep.* 2017;7(1):1-10.

53. Rusin P, Maxwell S, Gerba C. Comparative surface-to-hand and fingertip-to-mouth transfer efficiency of gram-positive bacteria, gram-negative bacteria, and phage. *J Appl Microbiol.* 2002;93(4):585-592.

54. Lopez GU, Gerba CP, Tamimi AH, Kitajima M, Maxwell SL, Rose JB. Transfer efficiency of bacteria and viruses from porous and nonporous fomites to fingers under different relative humidity conditions. *Appl Environ Microbiol*. 2013;79(18):5728-5734.

55. Julian T, Leckie J, Boehm A. Virus transfer between fingerpads and fomites. *J Appl Microbiol* 2010;109(6):1868-1874.

56. Duan M, Liu L, Da G, et al. Measuring the administered dose of particles on the facial mucosa of a realistic human model. *Indoor Air*. 2020;30(1):108-116.

57. Takahashi Y, Kato S, Yanagi U, Nagano H. Decrease in the number of bacteria for nucleic acid extraction and sampling of microbiome from the environment. *7th International Conference on Energy and Environment of Residential Buildings*, 2016:20-24.

58. Keeratipibul S, Laovittayanurak T, Pornruangsarp O, Chaturongkasumrit Y, Takahashi H, Techaruvichit P. Effect of swabbing techniques on the efficiency of bacterial recovery from food contact surfaces. *Food Control*. 2017;77:139-144.

59. Fábián TK, Hermann P, Beck A, Fejérdy P, Fábián G. Salivary defense proteins: their network and role in innate and acquired oral immunity. *Int J Mol Sci*. 2012;13(4):4295-4320.

60. Stephens B, Siegel JA, Novoselac A. Operational characteristics of residential and light-commercial air-conditioning systems in a hot and humid climate zone. *Build Environ.* 2011;46(10):1972-1983.

61. Kunkel S, Azimi P, Zhao H, Stark B, Stephens B. Quantifying the size-resolved dynamics of indoor bioaerosol transport and control. *Indoor Air.* 2017;27(5):977-987.

Figure legends:

Figure 1. Schematic of the experimental setup in the chamber. HP: healthy person, IP: infected person, PV: personalized ventilation

Figure 2. Schematic of different head orientations (a) L24, (b) L12, (c) H0, (d) H12, (e) H24, (f) R12 and R24. HP: healthy person, IP: infected person, PV: personalized ventilation

Figure 3. The sampling locations (a) on the HP's face and body, and (b) the detail information on the face. HP: healthy person

Figure 4. Visualization of the cough jet under H0 case without PV

Figure 5. (a) Visualization of the cough jet under H12 case without PV; (b)Visualization of the cough jet influenced by PV flow under H12 case

Figure 6. Deposition density of viable bacteriophages deposited on the HP's upper body and face under cases of (a) L24-H24 and (b) H0-R24

Figure 7. Deposition density on the HP's (a) chin, (b) mucous membranes, (c) cheek, (d) forehead under the cases of L24, L12, H0, H12, H24, and R12 with and without PV. Note: For R24 case, just few viruses deposited on the shoulder and forehead and no virus was found on other places. The performance of the PV flow of the R24 case was not investigated.

Figure 8. Deposition density on the HP's (a) chest, (b) shoulder, (c) neck under the cases of L24, L12, H0, H12, H24, and R12 with and without PV

The Effect of Head Orientation and Personalized Ventilation on Bioaerosol Deposition from a Cough

Running title: Head orientation & PV role in deposition

Jingcui Xu[1,2], Cunteng Wang[1,3], Sau Chung Fu[3], Christopher Y. H. Chao[3,4]

[1]Department of Mechanical and Aerospace Engineering, The Hong Kong University of Science and Technology, Hong Kong, China

[2]Department of Civil and Environmental Engineering, The Hong Kong Polytechnic University, Hong Kong, China

[3]Department of Mechanical Engineering, The University of Hong Kong, Hong Kong, China

[4]Department of Building Environment and Energy Engineering, Department of Mechanical Engineering, The Hong Kong Polytechnic University, Hong Kong, China

Correspondence

Sau Chung Fu, Department of Mechanical Engineering, The University of Hong Kong, Hong Kong, China. Email: scfu@hku.hk

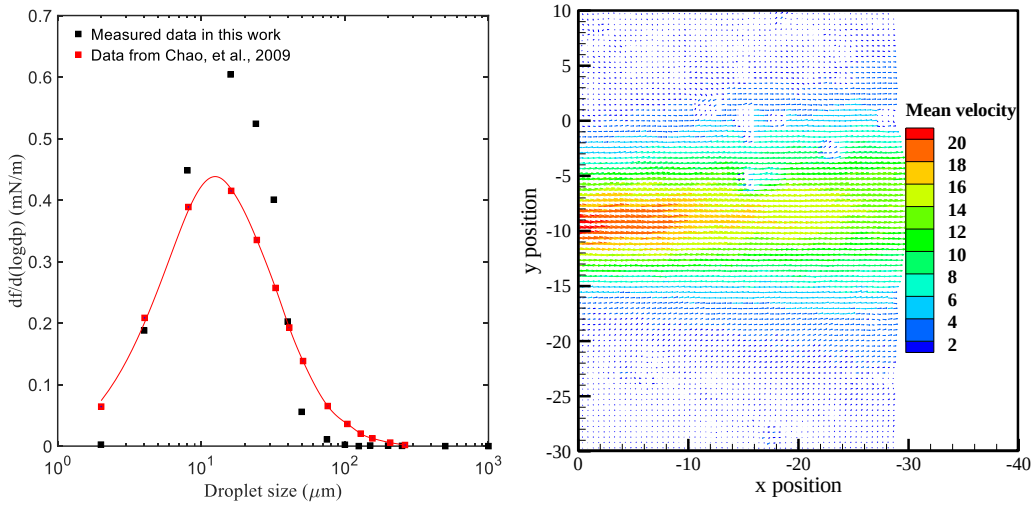

Figure 1S. Size distribution and velocity of aerosols released from the cough generator; The detailed measurement process can be found in the previous study [1].

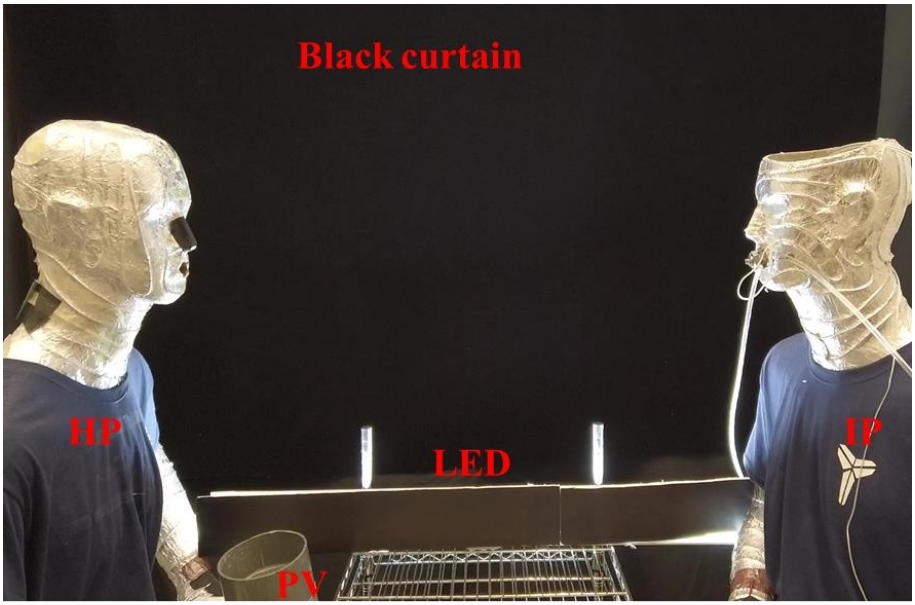

Figure 2S. Design for the visualization experiment. HP: healthy person, IP: infected person, PV: personalized ventilation

Figure 3S. Visualization of the cough jet under H24 case without PV

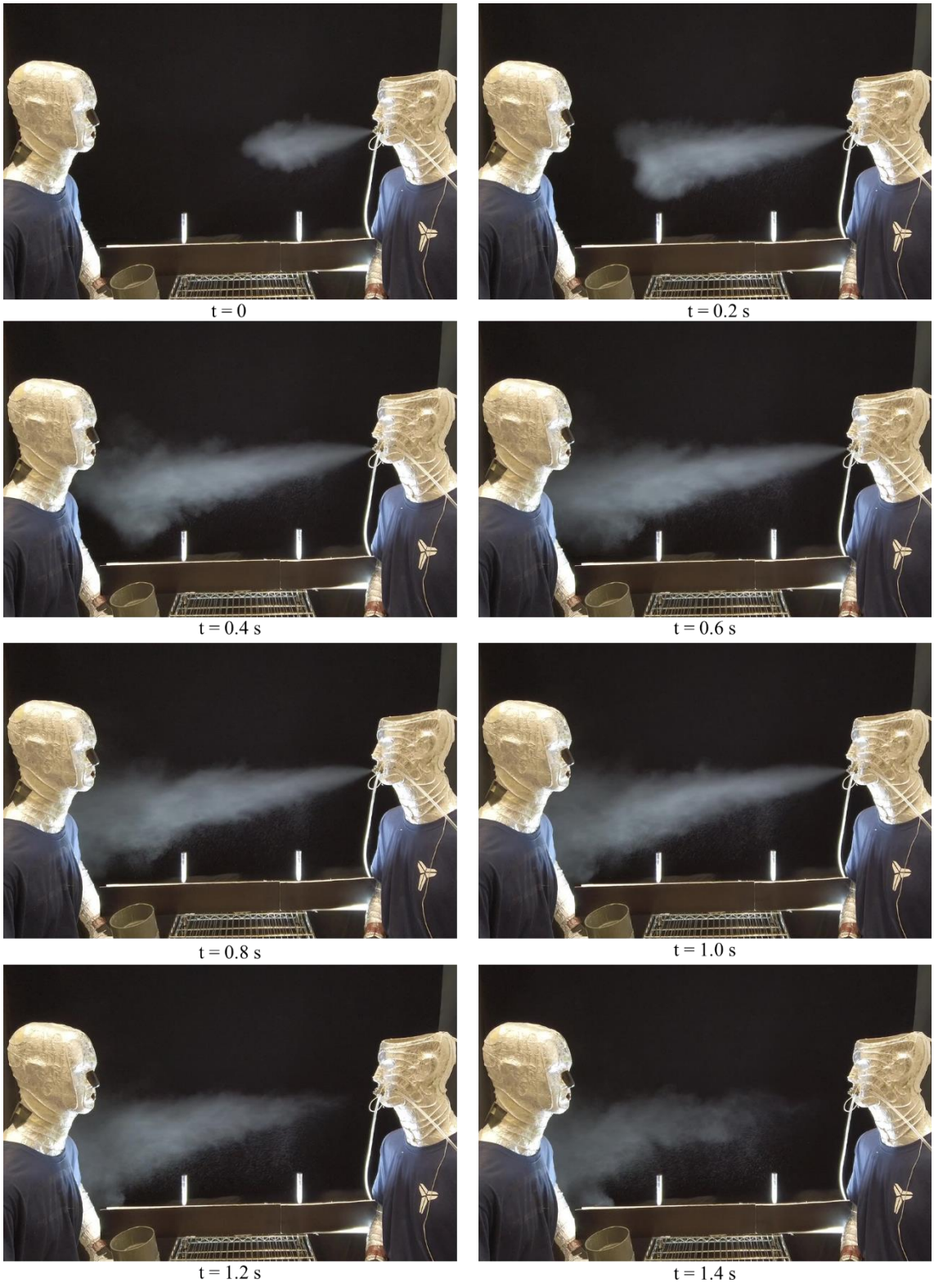

Figure 4S. Visualization of the cough jet under L12 case without PV

Figure 5S. Visualization of the cough jet under L24 case without PV

Figure 6S. Visualization of the cough jet under H24 case with PV

Cultivation methods

Bacteriophage T3 (ATCC 11303-B3) and the host *Escherichia coli* (ATCC 11303) with a safety level of one was used. For the host *E. coli* solution: A pure culture of *E. coli* was obtained by the streak plate method, and then a colony forming unit (CFU) *E. coli* was transferredd in the TSB solution (30 g of Tryptone Soya Broth (TSB) powder for every 1 L of distilled water) and cultured in an incubator at 37 ^{o}C for around 24 h. A high titre bacteriophage solution was prepared before the experiment. A plaque forming unit PFU bacteriophage T3 was cultured in the *E. coli* host solution for 10 h in an incubator at 37 ^{o}C. Then the soft-agar overlay technique was used: 0.1 ml bacteriophage T3 solution was mixed with 0.3 ml *E. coli* solution in a tube and waited for 15 minutes. Then 3 mL soft agar (5 g of nutrient broth powder and 2 g of count plate agar for every 200 ml distilled water) was mixed with bacteriophage and *E.coli* solution in the tubes and then was poured on the prepared agar plates. When solidified, they were inverted and put in an incubator for 10 hours. After that, 2-3 droplets of $CHCl_3$ were dropped on these plates containing sufficient PFUs, and the plates were inverted for 10 min. Then, the plates were reinverted and 3ml albumin-dextrose-saline (ADS) solution (0.81 g NaCl, 5 g bovine serum albumin, 2 g anhydrous dextrose for every 100 ml distilled water) was put on each plate and left for 30 min. After that, the top layer of the plates was scraped off into a flask using a funnel. The flask was put in a 37 ^{o}C water bath and shaken for 60 min. The contents of the flask were centrifuged at 10,000 g (m/s^2, acceleration) for 15 min at 20 ^{o}C. Then the supernatant was collected and centrifuged again at 28,000 g for 30 min at 20 ^{o}C. The resulting supernatant was discarded, leaving a small pellet. The pellet was suspended in 0.5 ml Tris buffer (PH 7.4; 6.05 of Tris, 5.8 g of NaCl and 2 g of $MgSO_4 \cdot 7H_2O$ for every 1 L distilled water). The solution was stored at 4 ^{o}C. The detailed protocol can be found in reference [1,2].

The test process:

Before experiments, the possible potential interactions between silicone material and deposited bioaerosols was checked. Three pieces of samples (4 cm × 4 cm) for testing were prepared by cutting the clean silicone face masks used on the face, silicone samples used on the upper body part and Petri dishes respectively. Petri dish was used as a reference. 1 μl of the saliva solution with bacteriophage viruses was dropped on these three samples. Saline solution was used to wash the prepared samples for collection. The cultivation method was used to characterize the number of viruses on each sample. Results showed that there was almost no difference between the silicone face masks, silicone samples and Petri dishes.

References

1. Wang CT, Fu SC, Chao CYH. Short-range bioaerosol deposition and recovery of viable viruses and bacteria on surfaces from a cough and implications for respiratory disease transmission. *Aerosol Sci Technol*. 2021;55(2):215-230.

2. Kunkel S, Azimi P, Zhao H, Stark B, Stephens B. Quantifying the size-resolved dynamics of indoor bioaerosol transport and control. *Indoor Air*. 2017;27(5):977-987.